scientific reports

Check for updates

OPEN

Size-segregated content of heavy metals and polycyclic aromatic hydrocarbons in airborne particles emitted by indoor sources

E. Caracci[1], A. Iannone[1,2], F. Carriera[1,2], I. Notardonato[2], S. Pili[3], A. Murru[3], P. Avino[2], M. Campagna[3], G. Buonanno[1,4] & Luca Stabile[1]✉

Indoor air quality is negatively affected by the emission of different combustion sources releasing airborne particles and related particle-bound toxic compounds (e.g., heavy metals and polycyclic aromatic hydrocarbons). To date, very few studies focused on the chemical characterization of the airborne particles emitted by indoor sources were carried out; moreover, no data on their size-resolved chemical compositions are available. In the present study, an experimental analysis aimed at determining the size-segregated content of heavy metals and polycyclic aromatic hydrocarbons in airborne particles (including sub-micrometric ones) emitted by widely-used indoor combustion sources (i.e., incenses, candles, mosquito-coils, and cooking activities) was carried out. To this purpose, airborne particles were collected through an electric low-pressure impactor and were post-analyzed by means of chromatography–mass spectrometry and atomic emission spectrometry techniques. Results of the analyses showed that the chemical composition of the emitted particles is not invariant to the particle size, indeed, an important contribution of sub-micrometric particle range to the total mass of chemical compounds emitted by the sources was noticed. These findings also demonstrated that significant underestimations of particle-bound compounds depositing in the lungs could occur if size-dependent compositions are not adopted.

Guaranteeing an adequate indoor air quality represents one of the major modern-day challenges for technical and scientific communities involved in designing and managing indoor environments[1–3]. For decades the main design parameters of efficient buildings were energy efficiency and, in case, the protection from outdoor pollutants[4–6] whereas the possible health threat of indoor sources was mostly underestimated[7]. In fact, building occupants are not properly aware of the indoor air quality, of their exposure to pollutants and, consequently, of how much they contribute to reducing the indoor air quality through their habits and activities (e.g. using combustion sources, such as incenses, candles, etc.)[8,9].

Airborne particles were recognized as one of the main hazardous pollutants emitted by indoor sources due to their capability to cross the respiratory system, carrying toxic compounds, depositing in the deepest airways, and provoking negative health effects[10–12]. To date, the attention of the scientific community is shifting from super-micrometric particles, such as PM_{10} and $PM_{2.5}$ (defined as particle mass concentrations with diameters less than 10 and 2.5 μm, respectively), to sub-micrometric particles[13,14]. Indeed, airborne particle dynamics and composition are strongly affected by their size, with smaller particles recently recognized as most critical for human health[15–18]. Among the different airborne particle-bound toxic compounds, heavy metals (HMs) and polycyclic aromatic hydrocarbons (PAHs) were recognized as highly detrimental for human health. As an example, long-term exposure to HMs can cause several adverse health effects including human developmental retardation, kidney damage, etc.[19–22]. Analogously, exposure to PAHs can increase the risk of respiratory and cardiovascular diseases, cognitive development delay, genetic mutations, etc.[21,23–25]. Moreover, some HMs (e.g. As, Cd, Cr(VI), Ni) and PAHs are classified as Group 1 human carcinogens by the World Health Organization[26].

[1]Department of Civil and Mechanical Engineering, University of Cassino and Southern Lazio, Cassino, FR, Italy. [2]Department of Agricultural, Environmental and Food Sciences, University of Molise, Campobasso, Italy. [3]Department of Public Health, Clinical and Molecular Medicine, University of Cagliari, Cagliari, Italy. [4]International Laboratory for Air Quality and Health, Queensland University of Technology, Brisbane, QLD, Australia. ✉email: l.stabile@unicas.it

Since airborne particle chemical composition and dynamics are size-dependent[27], investigating the size-resolved chemical composition of the entire airborne particle size range[28,29], i.e. including also sub-micrometric particles, is a key research issue in view of a more detailed risk assessment related to the exposure to indoor-generated airborne particles[30–32].

Combustion sources are widely used worldwide in indoor environments for several purposes (from cooking activities to religious and esthetical purposes, e.g. incenses, candles and mosquito coils)[33–35]. The scientific community recently characterized most of these sources from physical and dimensional points of view also providing emission rates/factors in terms of particle number and mass. For example, $PM_{2.5}$ emission rates were found in the ranges 5–250 mg h^{-1}, 0.02–25 mg h^{-1}, and 36.2–88.6 mg h^{-1} for incenses, candles and mosquito coils, respectively[36–40], while particle number emission rates were in the range of $4.54–10.8 \times 10^{14}$ part h^{-1}, $4.07–4.85 \times 10^{13}$ part h^{-1}, $2.92–4.57 \times 10^{14}$ part h^{-1} for incenses, candles and mosquito coils, respectively[40]. Such large deviations of the data are likely due to the source composition, e.g. presence of scent additives, essential oils, fragrances, etc.[41]. Emission factor data for cooking activities were found extremely high as well (typically $> 10^{13}$ part. h^{-1} and > 1 mg h^{-1}) and present large deviations due to the several influence parameters, e.g. cooking method (frying, deep-frying, grilling, boiling, baking, etc.), cooking temperature, type of food (vegetable, fat), type of stove (gas, electric, etc.)[42–47]. All these combustion sources present particle number distribution modes in ultrafine range (< 100 nm), with large deviations due to above-mentioned influence parameters, and a high contribution of the sub-micrometric particles to the airborne particle mass emitted[40,42,43].

Studies focused on the chemical characterization of the airborne particles emitted by indoor sources are fewer; some studies revealed the presence of dibenzo-p-dioxins/dibenzofurans, PAHs and HMs during incense, candles and mosquito coil burning and cooking activities[39,41,45,48–56], nonetheless, the data provided are still scarce also considering the several parameters potentially affecting the emission. As an example, we recently carried out an innovative approach to evaluate the lung cancer risk related to airborne particles emitted by indoor sources[31] which relies upon particle and related carcinogenic compound emission rates of the sources: one of the main limitations we faced was the incomplete information on the chemical analysis of the particles emitted by such sources. Moreover, we also pointed out that detailed size-segregated chemical compositions of the particles emitted by indoor sources, currently not available, would be extremely important: they would avoid the oversimplifying assumptions considering the chemical composition of the emitted particles invariant to the particle size.

To summarize, even if the scientific literature has characterized the airborne particle emission rates of indoor sources, chemical characterization of such particles was poorly investigated; in addition, information on size-segregated content of HMs and PAHs in indoor-generated airborne particles, that would be extremely useful for proper risk assessments, is completely missing.

In the present study, the size-resolved chemical characterization of airborne particles emitted by indoor combustion sources, i.e. incenses, candles, mosquito-coils and cooking activities (grilling bacon), was carried out and size-dependent HM and PAH contributions to the PM_{10} were provided thanks to an experimental analysis based on airborne particle collection through an electric low-pressure impactor and consequent gas chromatography-mass spectrometry (GC–MS) and atomic emission spectrometry (AES) analyses.

Materials and methods

Emission sources and sampling site description

Particle sampling experiments were carried out at the Laboratory of Industrial Measurements (LAMI) of the University of Cassino and Southern Lazio, Italy. Samplings were performed in a 1.80 m × 1.20 m × 2.20 m plexiglass chamber presenting a small opening allowing supplying air for combustion phenomena as well as for electrical cables and ducts. The air exchange rate of the chamber in this condition was measured adopting a CO_2 decay method (not reported here for the sake of brevity[57]) and resulted equal to 0.50 ± 0.03 h^{-1}.

Four different emission sources were tested during the experimental campaign: candles, incense sticks, mosquito coils, and grilling bacon on an induction cooker. Candles, incenses, and mosquito coils commercially available were chosen. In particular, candles adopted in the experimental campaign were paraffin wax candles without any kind of additives, incenses were natural benzoin resin sticks, and mosquito coils were made up of prallethrin (pyrethroid insecticide) with co-formulants and colorants. The investigation of cooking activities was limited to the grilling of bacon (which represents one of the most emitting cooking activities[42]) on a portable induction cooker.

Particle sampling: apparatus description and procedure

In order to collect size-resolved mass amounts for post-hoc chemical characterizations, an electrical low-pressure impactor ELPI + ™ (Dekati Ltd.) was employed (it was placed inside the chamber, whereas its pump was placed outside) and polycarbonate collection foils (type 23,000, dim. 25 mm, Sartorius Stedim Biotech GmbH, Goettingen, Germany) were mounted at each ELPI stage. The ELPI + ™ is a particle spectrometer able to measure airborne particle number distribution (and total concentration) in real-time and simultaneously collect particles with a sampling flow rate of 10 L min^{-1}. Particles are firstly charged with a known charge level in a corona charger, then, they are size classified in a low-pressure cascade impactor according to their aerodynamic diameter. Every impactor stage is electrically insulated, and particles collected in each stage produce an electrical current proportional to particle number concentrations.

The ELPI + ™ presents 15 stages whose lower–upper boundary diameter ranges (expressed as 50% efficiency cut-off diameters, D_{50}) are: 6.0–16.7 nm for stage 1, 16.7–31.3 nm for stage 2, 31.3–54.7 for stage 3, 54.7–94.9 for stage 4, 94.9–156 nm for stage 5, 156–258 nm for stage 6, 258–384 nm for stage 7, 384–606 nm for stage 8, 606–952 nm for stage 9, 952 nm-1.64 µm for stage 10, 1.64–2.48 µm for stage 11, 2.48–3.67 µm for stage 12, 3.67–5.39 µm for stage 13, 5.39–9.93 µm for stage 14, 9.93–10 µm for stage 15. The upper boundary of stage

15 depends on the PM inlet sampling head adopted (if any); we have adopted an EN 12,341 PM_{10} inlet (down-scaled to 10 L min^{-1}), thus, as mentioned above, the upper diameter D_{50} of the stage 15 is actually 10 µm. Stage 1 (6.0–16.7 nm) doesn't allow particle collection, whereas stage 15 (9.93–10 µm) acts as a pre-cut stage thus, it is not measured electrically.

Since HM and PAH determination was performed separately, adopting different methods and instruments, two different samplings were performed for chemical post-analyses: Sampling 1 for HMs and Sampling 2 for PAHs. As concern the source combustion, candles were normally burnt, while incenses and mosquito coils were lit by a flame and fanned out so that the glowing ember continued to smolder and burn away the rest of the materials. Grilling of bacon was performed by putting the bacon slices on a pan heated by an induction cooker. In order to collect an adequate amount of particle mass on each ELPI + ™ stage for chemical post-analyses high mass concentrations for long periods were needed. To this end preliminary tests were carried out to check the concentrations reached and estimate the number of sources to burn simultaneously and the total sampling period. Then, the following procedure for each indoor source and each sampling was adopted: several sources (e.g. candles) were lit up simultaneously and the particle collection and measurement with the ELPI + ™ was started as well, then, when the sources burnt out (or, in the case of the cooking activity, when the bacon was properly grilled), they were replaced with new ones. This procedure was performed several times for each source: the quantity of source burnt, the total sampling period, and the average number and mass concentrations measured by the ELPI + ™ during the samplings are summarized in Table 1 for each source type for both the samplings.

To avoid any contamination between the sources, the charger and the impactor of the ELPI + ™ were cleaned according to the manufacturer suggestions at the end of each sampling and flush pump was used to keep the ELPI + ™ clean between the measurements. Moreover, surfaces of the chamber were cleaned to avoid contamination between the sources due to resuspension of previously deposited particles. Finally, in order to minimize the contribution of particles coming from the environment outside the chamber, a fan filter unit equipped with a HEPA H14 filter and a F7 pre-filtration stage was used at the maximum flow rate of 850 m^3 h^{-1} to clean the environment before test. Nonetheless, in order to avoid measurement artifacts, two further samplings were performed to determine the possible presence of HMs and PAHs in the chamber when the sources are not in operation. These samplings (referred as Sampling blank 1, for HMs, and blank 2, for PAHs) were performed after having applied the abovementioned cleaning procedures (i.e. cleaning of the chamber surface and filtration of the ambient air of the chamber through the fan filter unit), both the samplings were carried out for 10 h consecutively. Concentrations of HMs and PAHs resulting from the analysis of particle mass collected during Sampling blank 1 and blank 2, respectively, resulted lower than the LODs, then guaranteeing that the HM and PAH determination due to the use of combustion sources was not affected by the presence of pre-existing airborne particles in the chamber.

HM determination: apparatus description and analytical method

The analysis of HMs in particle mass samples (Sampling 1 and Sampling blank 1) involved a preliminary digestion of polycarbonate filters in a microwave digestion system (Mars 5, CEM Corporation, Mathews, North Carolina, USA). The protocol applied was as follows: filters were transferred into Autovent HP-1500 vessel and digested with 10 mL of HNO_3 according to the instrumental parameters previously set (600 W, 100% Power, 20 min). The digested solution obtained was diluted with ultrapure water (1:10 v/v) before the analysis (detailed information about chemicals and reagents is reported in the Supplementary Information). Heavy metal extract concentrations were determined by Inductively Coupled Plasma—Atomic Emission Spectroscopy using Agilent Technologies 4210 MP-AES Atomic Absorption Spectrometer (AAS). The MP-AES method was validated by the construction of calibration curves in the linear range of 0.05–5 ng mL^{-1}. A multielement mix of heavy metals was used as a standard solution. The emission wavelengths selected for each metal analyzed were: 228.802 nm for Cd, 425.433 nm for Cr(VI), 324.754 nm for Cu, 405.781 nm for Pb, 231.147 nm for Sb, 213.857 nm for Zn, 193.695 nm for As, 340.512 nm for Co, 403.076 nm for Mn, and 361.939 nm for Ni. The limit of detection (LOD) and limit of quantification (LOQ) of the method for heavy metal determination are reported in Table S1 (please see Supplementary Information).

PAH determination: apparatus description and optimization and validation of the analytical method

The amount of PAHs in particle mass samples (Sampling 2 and Sampling blank 2) collected on polycarbonate filters was extracted by ultrasonic extraction (USAE) procedure. The protocol was performed as follows: filters

Source type	Quantity		Total sampling period (min)		Average particle number concentration (part. cm^{-3})		Average PM_{10} concentration (mg m^{-3})	
	Sampling 1	Sampling 2	Sampling 1	Sampling 2	Sampling 1	Sampling 2	Sampling 1	Sampling 2
Candles	24 candles	32 candles	889	628	1.68×10^6	1.35×10^6	31.0	60.3
Incenses	10 sticks	10 sticks	246	246	3.81×10^6	3.00×10^6	462.0	353.0
Mosquito Coils	4 coils	2 coils	458	347	8.32×10^6	9.07×10^6	43.7	77.4
Grilling bacon	1 kg	1 kg	727	486	6.68×10^5	9.15×10^5	6.9	31.8

Table 1. Quantity of sources burnt, total sampling period, average particle number and mass concentrations for each sampling and for each source type (Sampling 1 for HM analysis, Sampling 2 for PAH analysis).

were placed in a beaker, covered with 2 mL of n-heptane solvent and extracted in an ultrasonic bath (Ultrasounds Starsonic 18–35, Liarre s.r.l, Casalfiumanese, Italy) for 6 min at room temperature for three times. The final extracts were combined in the same vial, dried under the stream flow of nitrogen, and recovered with 500 µL of n-heptane before the GC–MS analysis. A mix solution of 15 PAHs was used as a laboratory standard to evaluate the feasibility and reproducibility of the analytical method proposed (detailed information about chemicals and reagents are reported in the Supplementary Information). PAHs were quantified by means of GC-Ion-Trap MS (GC-IT/MS) analysis using a gas chromatograph Finnigan Trace GC Ultra (ThermFinningan, Bremen, Germany) equipped with a Polaris Q ion trap mass spectrometry detector (Thermo Fisher Scientific, Waltham, MA). The column Meta-XLB™ (30 m length, 0.25 mm internal diameter, 0.25 µm film thickness; Teknokroma™, Barcelona, Spain) was used for the separation, and He (99.9995% purity) was adopted as carrier gas at a flow rate of 1.0 mL min^{-1}. The sample injection (V_{inj} = 1 µL) was performed in splitless mode with an opening split for 4 min through AI/AS 1310 autosampler. After the injection, the Programmed Temperature Vaporizer (PTV) injector heated from 110 to 320 °C at 800 °C min^{-1}. In order to ensure the cleanup of the line, the injector was kept at 320 °C for 10 min after the sample vaporization. The starting oven temperature was 100 °C held for 30 s, then, it was ramped to 150 °C at 20 °C min^{-1} for 2 min and to 290 °C at 20 °C min^{-1} for 10 min. Before the chromatographic separation of PAHs, an internal standard solution of dioctyl phthalate (DOP) at 1 ng μL^{-1} was added to the samples.

Detection of PAHs was achieved in selected ion monitoring (SIM) with detector temperature and transfer line set at 250 °C and 270 °C, respectively. Full-scan MS data were acquired over the mass-to-charge (*m/z*) ratio ranging from 100 to 400 amu to obtain the fragmentation spectra of the analytes while Thermo Xcalibur Sequence Setup software was used for the data interpretation. The mass-to-charge (*m/z*) ratios and retention times of PAHs identified by GC–MS are reported in Table S2 (please see Supplementary Information). The method adopted was standardized through the construction of calibration curves in linear ranges reported in Table S2 as well. Recoveries of PAHs from samples spiked with standard solution were found in the range of 87–98% with the error ranging between 8–15%. The limits of detection (LOD) and limits of quantification (LOQ) of the method for PAH determination are summarized in Table S2.

Data post-processing

Calculation of the particle and chemical compound concentrations

Data post-processing of particle distributions and total concentrations was performed through the $ELPI_{VI}$ software. Particle mass distribution and total concentration were evaluated on the basis of the number distribution data and applying the following particle densities: 1.1 g cm^{-3} for incenses and mosquito coils[50,58,59], 1.5 g cm^{-3} for candles[39], and 1.0 g cm^{-3} for grilling of bacon[43,60]. Moreover, corrections for diffusion and space charger losses were applied[61]. Results of particle mass distributions and concentrations hereinafter reported, were obtained by averaging values of the sampling periods (Sampling 1 and 2) for each source.

We also point out that, since mass concentrations at stage 15 are not available (and the stage width is much smaller than others; please see section "Particle sampling: apparatus description and procedure"), in this paper, we are referring to PM_{10} as the mass concentration in the range 16.7 nm–9.93 µm. Similarly, we are referring to PM_1 as the mass concentration in the range 16.7 nm–952 nm.

HMs and PAHs particle mass distributions were obtained as follows: (a) firstly, HM and PAH absolute masses (ng) were calculated by multiplying the concentrations in the solution (i.e. extract concentration; expressed with respect to the solution volume, ng mL^{-1} or ng μL^{-1}) by the solution volume, 10 mL and 500 µL, for HMs and PAHs, respectively, (b) then, they were divided by the total sampling volume (depending on ELPI + ™ flow rate, 10 L min^{-1}, and sampling periods summarized in Table 1).

Mass fraction of the HMs and PAHs on PM_{10} emitted by the different sources were evaluated as well as particle mass distributions, such distributions were normalized with respect to the corresponding total mass concentrations then obtaining relative particle mass distributions.

Estimation of the deposited concentration of chemical compounds

The knowledge of the size-resolved chemical composition of airborne particles emitted by the indoor sources under investigation also allows a proper estimate of the actual dose of chemical compounds received by exposed people and the related health risks. Indeed, thanks to the size-resolved chemical composition, size-dependent mass fractions of chemical compounds can be applied; consequently, the oversimplifying assumption considering the chemical composition of the emitted particles invariant to the particle size (i.e. constant mass fraction on the entire particle size range) can be superseded. To this end, as an example, we have evaluated the deposited concentration of chemical compounds (i.e. the dose per unit inhalation rate and unit time of exposure) that an exposed person can receive when exposed to the airborne particles emitted by the sources under investigation considering two different approaches: (a) actual amount of chemical compounds per each channel, i.e. mass fraction obtained from the measured size-resolved mass distributions of the compounds, (b) constant chemical composition for each particle size, i.e. constant measured mass fraction of the compounds (i.e. those reported in Tables 2 and 3). The ratio between the deposited concentrations ($dM_{j\text{-}dep}$) evaluated according the two different methods (size-resolved, SR, and constant, CONST) of the *j*-th chemical compound received by an exposed person for a specific indoor source can be evaluated as:

$$R_j = \frac{dM_{j-dep\_SR}}{dM_{j-dep\_CONST}} = \frac{\sum_i \left(\frac{dM}{dlogD_p}\right)_i \cdot dlogD_{p,i} \cdot MF_{j,i} \cdot DF_i}{MF_j \cdot \sum_i \left(\frac{dM}{dlogD_p}\right)_i \cdot dlogD_{p,i} \cdot DF_i} \quad (1)$$

HMs	Candles	Incenses	Mosquito coils	Grilling bacon
As	–	–	2.93×10^{-6}	5.95×10^{-6}
Cd	–	–	1.04×10^{-6}	2.14×10^{-5}
Cr(VI)	–	–	2.43×10^{-5}	4.16×10^{-6}
Ni	–	–	8.93×10^{-7}	–
Pb	4.21×10^{-6}	1.65×10^{-6}	9.57×10^{-6}	1.59×10^{-5}
Sb	2.88×10^{-5}	7.18×10^{-6}	6.32×10^{-5}	5.35×10^{-6}
Cu	1.15×10^{-5}	4.23×10^{-6}	6.50×10^{-6}	6.23×10^{-5}
Zn	4.78×10^{-5}	1.88×10^{-5}	3.13×10^{-5}	9.10×10^{-5}
Co	–	–	–	1.98×10^{-7}
Mn	4.96×10^{-7}	–	–	–

Table 2. Mass fractions of HMs on PM_{10} (expressed as ng ng^{-1}) in the freshly emitted particles by the indoor sources under investigation.

PAHs	Candles	Incenses	Mosquito coils	Grilling bacon
Acenaphthylene	–	6.65×10^{-7}	–	–
Acenaphthene	–	6.16×10^{-7}	–	–
Fluorene	–	–	–	3.39×10^{-6}
Phenanthrene	2.56×10^{-6}	3.25×10^{-6}	3.86×10^{-6}	4.03×10^{-6}
Anthracene	1.34×10^{-6}	9.51×10^{-7}	1.67×10^{-6}	1.94×10^{-6}
Fluoranthene	5.10×10^{-6}	2.66×10^{-6}	8.24×10^{-6}	3.63×10^{-6}
Pyrene	2.38×10^{-6}	1.62×10^{-6}	3.82×10^{-6}	2.65×10^{-6}
benzo(a)anthracene	–	–	–	–
chrysene	1.63×10^{-6}	1.28×10^{-6}	4.20×10^{-6}	2.27×10^{-6}
Benzo(b)fluoranthene	2.93×10^{-6}	1.77×10^{-6}	6.82×10^{-6}	5.65×10^{-6}
Benzo(k)fluoranthene	–	–	–	–
Benzo(a)pyrene	–	2.14×10^{-6}	4.77×10^{-6}	3.15×10^{-6}
Indeno(1,2,3-cd)pyrene	–	–	–	–
Dibenzo(a,h)anthracene	–	–	–	–
Benzo(g.h.i)perylene	–	–	–	–

Table 3. Mass fractions of PAHs on PM_{10} (expressed as ng ng^{-1}) generated by the indoor sources under investigation.

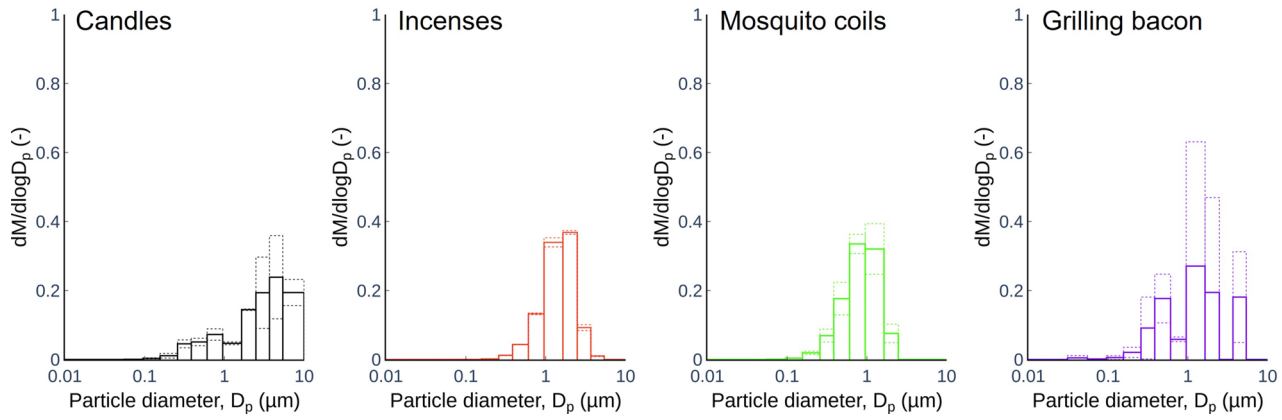

Fig. 1. Particle mass distributions, normalized to the total concentration, measured during combustion of candles, incenses, mosquito coils, and grilling bacon through the ELPI + ™: solid lines represent average distributions, dashed lines represent standard deviations of the measured distributions.

where $(dM/dlogD_p)_i$ represents the particle mass concentration of the i-th channel size measured for the specific source under investigation (as reported in Fig. 1), $dlogD_{p,i}$ is the width of the i-th channel, $MF_{j,i}$ is the mass fraction of the j-th chemical compound measured for the i-th channel size (needed for SR case), DF_i is the deposition fraction of particles in the lungs (sum of deposition in the alveolar and tracheobronchial regions) as a function of their size, MF_j is the constant mass fraction the j-th chemical compound (needed for CONST case). The DF_i values were obtained from the International Commission on Radiological Protection[62], in particular, we considered average curves between adult males and females (normal nose breather, sitting activity).

Results and discussions

Particle mass distributions

Particle mass distributions averaged among the two samplings (Sampling 1 for HM analysis and Sampling 2 for PAH analysis) for the sources under investigation are shown in Fig. 1, distributions are presented as relative distributions, i.e. normalized to the total mass concentration measured during the samplings. For all the sources a not negligible contribution of PM_1 fraction was recognized, in particular, the average PM_1 fractions with respect to PM_{10} were equal to 18%, 18%, 57%, and 35% for candles, incenses, mosquito coils, and grilling bacon, respectively.

Candles present a bimodal distribution with a main mode at stage 13 (3.67–5.39 μm) and a second minor mode in the sub-micrometric range (at stage 9, 606–952 nm), on the contrary incenses are characterized by an unimodal distribution with a main mode at stage 11 (1.64–2.48 μm). Mosquito coils produced an unimodal mass distribution as well with a mode in the sub-micrometric range (at stage 9, 606–952 nm). Finally, the mass distribution related to grilling bacon resulted bimodal with a main mode in the super-micrometric range (at stage 10, 952 nm–1.64 μm) and a secondary mode in the sub-micrometric range (at stage 8, 384–606 nm).

Actually, very few studies reporting mass distribution of freshly emitted particles from indoor combustion sources were carried out by the scientific community. Particle mass distributions while cooking were measured through an ELPI by See and Balasubramanian[63] in a Chinese-cooked food stall fueled by LPG, they recognized a bimodal distribution similar to that here presented. In our previous papers, we measured particle mass distributions indoor by adopting an SMPS-APS system while grilling bacon on a gas stove[43] and while using candles, incenses and mosquito coils[40]: distributions for grilling bacon resulted quite similar to those measured in this paper, whereas a smaller mode (about 300 nm) was measured for candles, incenses and mosquito coils. Such variation can be likely due to the huge variability in the composition of the sources.

HM and PAH concentrations

HMs

The results of the analysis of heavy metals in freshly emitted particles by candle, incense, and mosquito coil combustions, and grilling bacon are summarized in Table S3 (please see Supplementary Information) where heavy metal extract concentrations (ng mL^{-1}) analyzed by ICP-AES are shown. The data highlight the presence of Group 1 carcinogenic compounds, i.e. As, Cd, Cr(VI), Ni, in particle samples from mosquito coil combustion and grilling bacon, whereas in samples obtained from candle and incense combustions, they resulted below the limit of detection (LOD). On the contrary, the presence of Cu, Pb, Zn, Sb was recognized in particle samples collected for all the sources under investigation. In addition, traces of Mn were detected only in particle samples collected during candle combustion, whereas Co only was found in samples collected while grilling bacon.

From these data, and adopting the data post-processing described in "Data post-processing", the HM mass fractions on PM_{10} (expressed as ng ng^{-1}), were calculated and reported in Table 2: the calculated mass fractions were quite high as they were mostly in the 10^{-6}–10^{-5} range, i.e. values similar to those typically found in outdoor urban environments[30,64,65]. A proper comparison with the few data available in the literature cannot be carried out: indeed, the presence of HMs during the combustion of such indoor sources was previously identified[39,45,48,56,66] but, even if HM concentrations were provided, the corresponding PM_{10} were not[67]. This is the main difficulty we also experienced in our previous paper[31] where mass fractions of toxic compounds (with respect to PM_{10}) were needed to properly estimate the lung cancer risk in indoor environments. Actually, we reported mass fractions of carcinogenic compounds (Group 1) on PM_{10} emitted by wood and pellet combustion phenomena[68]; nonetheless, no exhaustive studies were available for other indoor sources here investigated.

Despite their overall contribution to the total particle mass a further key information is evaluating the size-resolved mass distribution of HMs. Indeed, as mentioned above, different sizes imply different ability of particles to penetrate in the lungs and transporting there such compounds. In Fig. 2 mass distributions of As, Cd, Ni, Cr(VI) (Group 1 carcinogenic HMs) and Pb, Sb, Cu, Zn in freshly emitted particles from mosquito coil combustion (Sampling 1) are shown. The distributions clearly show that the amount of As is exclusively present in the ultrafine particle range with a huge contribution in stage 2 (16.7–31.3 nm). Similarly, Ni contribution is exclusively due to the sub-micrometric particle range (stages 6 and 7) with a main peak in the 156–384 nm range. Cr(VI) contribution as well was almost completely related to sub-micrometric particles with a clear peak in the range 156–384 nm, whereas the sub-micrometric particle range contribution to the total amount of Cd is 67% as the distribution resulted unimodal with a peak in stage 9 (606–952 nm). As concerns Pb, Sb, Cu and Zn the sub-micrometric contributions are 48%, 64%, 26%, and 11%, respectively; in particular, the Pb mass distribution is unimodal with a main peak at 606–952 nm, the Sb distribution is almost uniform, Cu distribution presents two modes, one in the sub-micrometric (94.9–156 nm) and the other in the super-micrometric range (1.64–2.48 μm), whereas Zn is unimodal with a mode in the super-micrometric range (1.64–2.48 μm).

In Fig. 3 mass distributions of As, Cd, Cr(VI) and Pb, Sb, Cu, Zn, Co in freshly emitted particles from grilling bacon (Sampling 1) are shown. As and Cd present a contribution of a sub-micrometric range equal to 67% and 61%, respectively, with a significant fraction in the ultrafine range (around 30% of their total mass), whereas

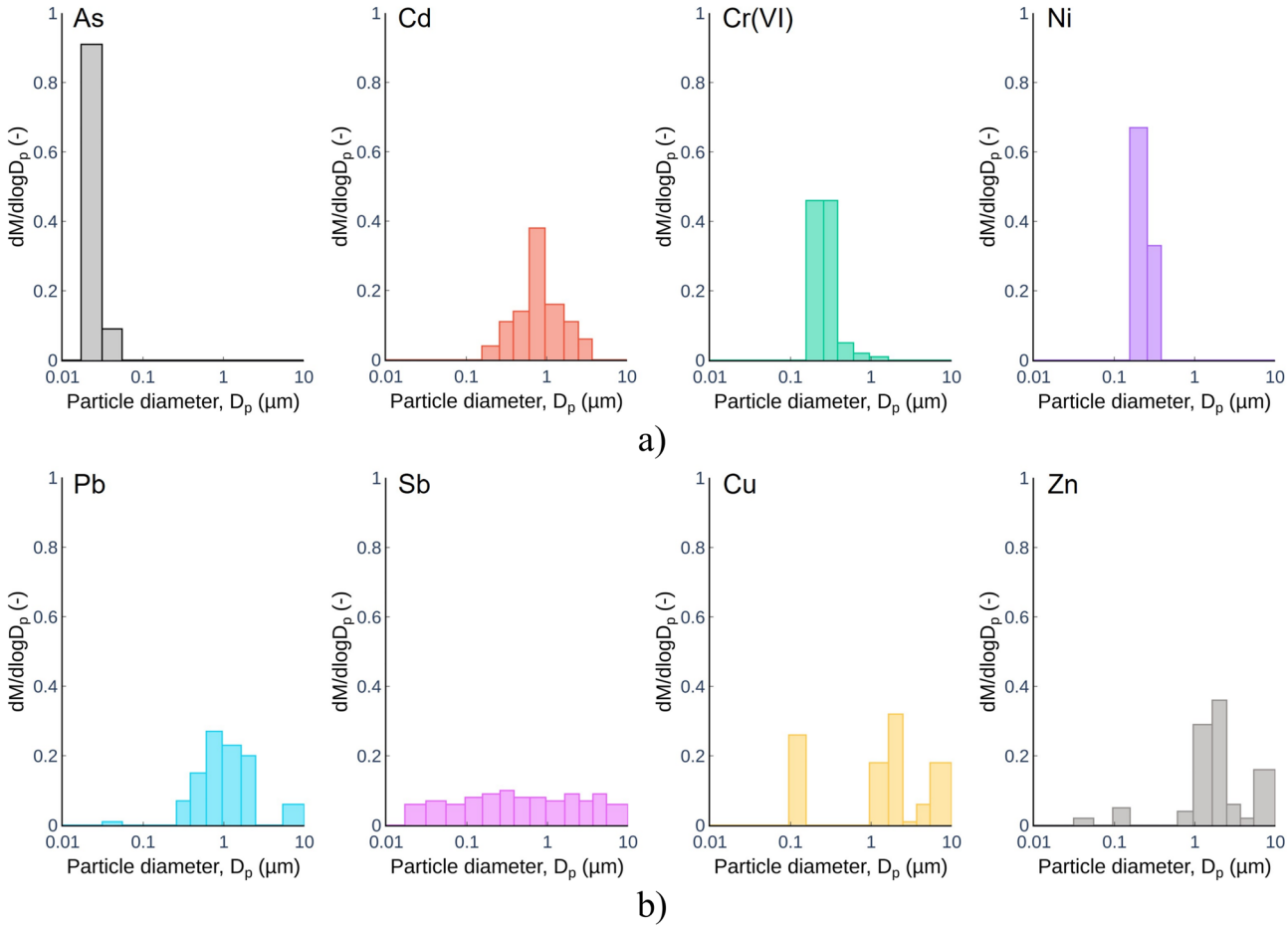

Fig. 2. Mass distributions (normalized to the total concentration) of As, Cd, Cr(VI), Ni (**a**) and Pb, Sb, Cu, Zn (**b**) in freshly emitted particles from mosquito coils combustion (Sampling 1).

Cr(VI) is almost exclusively present in the sub-micrometric range (95%) as it shows a main peak of the mass distribution in the range 31.3–54.7 (stage 3). As concerns the other compounds, a contribution of the sub-micrometric range of about 70% was detected for Pb, Sb, and Cu, whereas it is equal to 83% for Zn and 100% for Co (completely included in stage 4).

Pb, Sb, Cu, Zn and Mn mass distributions in freshly emitted particles from candle and incense combustion experiments are reported in Fig. 4; such distributions resulted quite uniform with sub-micrometric range contributions to their total masses around 60%; with the exception of Mn for candles whose contribution is completely due to the sub-micrometric range (main mode at 384–606 nm).

We point out that the huge contribution of the sub-micrometric particle range emitted by mosquito coil combustion and grilling bacon is a critical aspect in terms of people's exposure and related lung cancer risk since As, Cd, Ni, Cr(VI) represent the particle-bound compounds with the highest inhalation cancer slope factors[69].

As mentioned above, size-resolved chemical compositions of airborne particles sampled in indoor environments or emitted from indoor sources are not common in the scientific literature. In a recent paper Martins et al.[70] provided size-resolved chemical compositions of PM_{10} sampled both at outdoor and indoor environments of schools and homes: in this study, the presence of the HMs in sub-micrometric particle range was also detected, with some differences between schools and homes likely due to the different sources affecting such environments (mainly penetration from outdoor for schools, possible presence of indoor sources for homes). Similarly, Pekey et al.[71] found a higher presence of some HMs in homes with respect to outdoor values due to the possible presence of indoor sources (especially in winter when indoor-generated pollutants can slowly exfiltrate). Nonetheless, in these papers, the contribution of indoor sources to such indoor chemical compound concentrations is not provided.

PAHs

Results of the analysis of PAHs in freshly emitted particles due to the combustion of the investigated sources are reported in Table S4 (please see Supplementary Information) where PAH extract concentrations are summarized. Particle samples collected during the combustion experiments showed the presence of several PAHs emitted by the sources under investigation; in particular, benzo(a)pyrene which is classified as Group 1 carcinogenic compound was detected during incense and mosquito coil combustion as well as grilling bacon experiments. Group

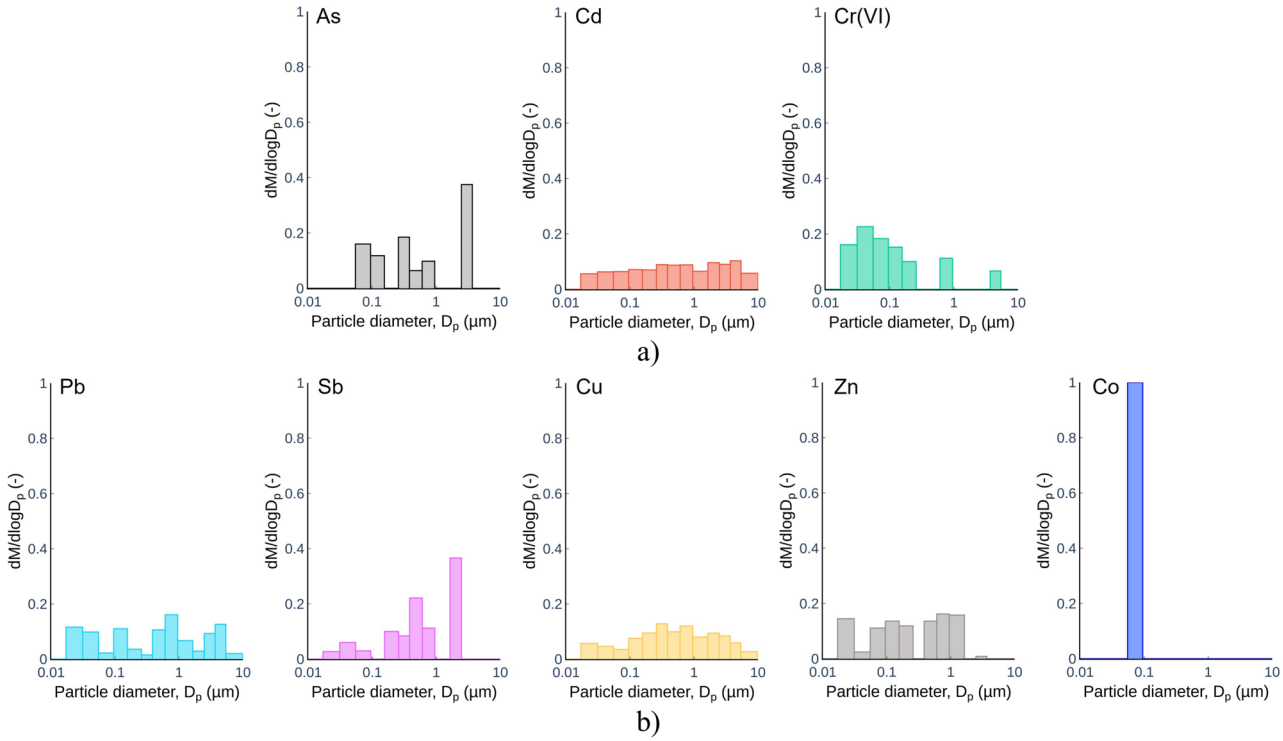

Fig. 3. Mass distributions (normalized to the total concentration) of As, Cd, Cr(VI) (**a**) and Pb, Sb, Cu, Zn, Co (**b**) in freshly emitted particles from grilling bacon (Sampling 1).

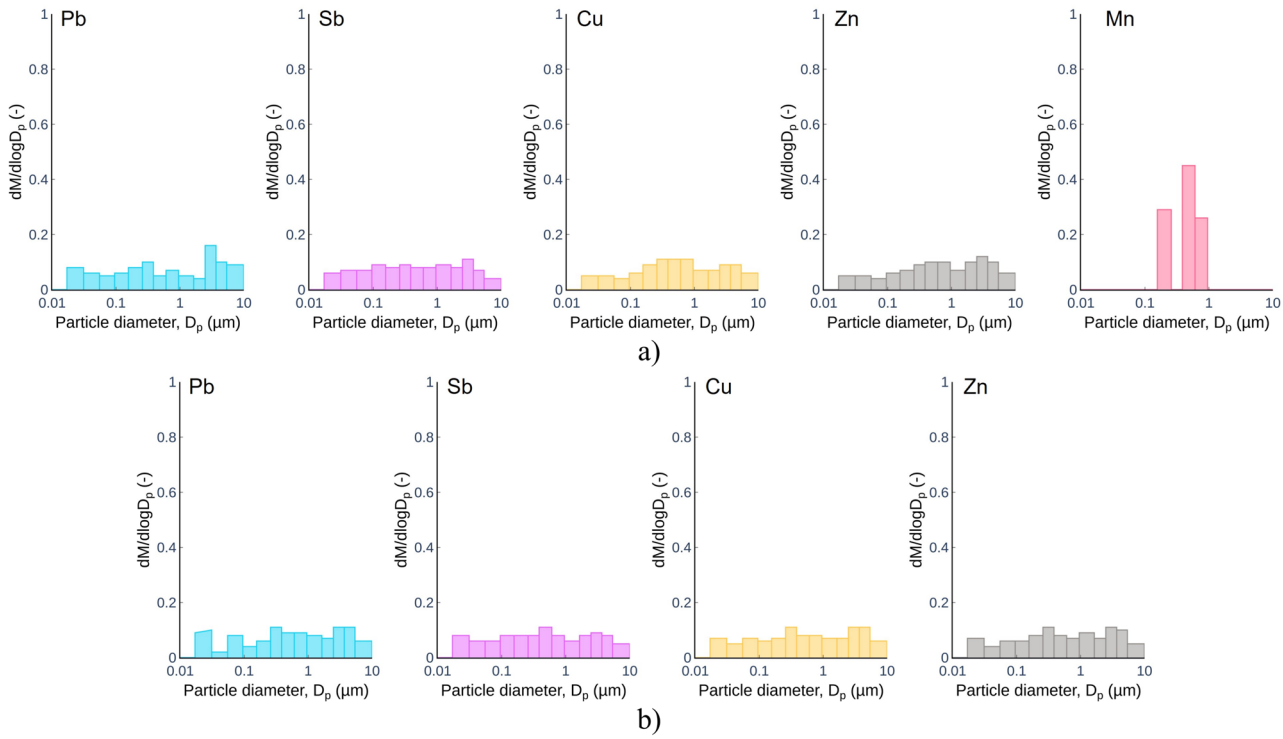

Fig. 4. Mass distributions (normalized to the total concentration) of Pb, Sb, Cu, Zn and Mn in freshly emitted particles from candle (**a**) and incense (**b**) combustions (Sampling 1).

2 carcinogenic compounds (e.g. chrysene, benzo(b)fluoranthene) and three- (fluorene, phenanthrene) and four-ring PAHs (fluoranthene, pyrene), which are classified as Group 3 carcinogenic compounds (i.e. not classifiable due to insufficient information)[69], were also detected. On the contrary, for all the investigated indoor sources concentrations of benzo(a)anthracene, indeno(1,2,3-cd)pyrene, dibenzo(a,h)anthracene, benzo(k)fluoranthene, and benzo(g.h.i)perylene resulted under of the limit of detection (LOD). PAH mass fractions on PM_{10} (expressed as ng ng^{-1}), calculated as described in the section "Data post-processing", are reported in Table 3. Such values ranged between 10^{-7} and 10^{-5} which are, again, not negligible and similar to those typically measured at outdoor urban sites[72]. As already mentioned for HMs, a proper comparison with the few data available in the literature cannot be carried out. Indeed, even if PAHs were measured in cooking-generated particles[66], during candle burning event[41], incense burning event[67], and mosquito coils burning event[53], the mass factions and size-resolved analyses were not provided.

In Fig. 5 mass distributions (normalized to the total concentration) of detected PAHs in freshly emitted particles from candle, incense, mosquito coil combustions and grilling bacon are reported. Particles emitted by candles present a predominant contribution of sub-micrometric range, indeed such sub-micrometric contributions for phenanthrene, anthracene, fluoranthene, pyrene, chrysene, benzo(b)fluoranthene resulted equal to 80%, 88%, 75%, 75%, 76%, and 65%, respectively, with a not negligible contribution (except for benzo(b)fluoranthene) of the ultrafine particle range (25–38%). For incenses, the contribution of the sub-micrometric range to the total mass of the emitted PAHs resulted in the range 43–50%. In particular, 46% of benzo(a)pyrene mass, which is the most critical PAH for human health, was detected in the sub-micrometric range. Benzo(a)pyrene was also detected in particles generated by mosquito coil combustion and grilling bacon with sub-micrometric particle contributions of 67% and 100%, respectively. Particles released from mosquito coil combustion also showed the presence of phenanthrene, anthracene, fluoranthene, pyrene, chrysene, and benzo(b)fluoranthene (with the contribution of the sub-micrometric particles from 56 to 80%). Similarly, a huge contribution of the sub-micrometric range (54–100%) was also detected for other PAHs emitted by grilling bacon (fluorene, phenanthrene, anthracene, fluoranthene, pyrene, chrysene, benzo(b)fluoranthene).

Estimated deposited concentration of chemical compounds

The results provided in the present study represent a novel finding since mass fractions and size-resolved chemical compositions of airborne particles emitted by some widely-used indoor sources are shown for the very first time. This is a key information in view of a more detailed analysis of the indoor air quality and related risk assessment. Indeed, a direct implication of the data here shown is the different deposited concentrations of compounds in the lungs when adopting actual mass distribution of the compounds. To this end, in Table 4 the ratios between the deposited concentrations, evaluated according to the two different methods (size-resolved and constant), calculated according to the Eq. 1 and the hypothesis of the section "Estimation of the deposited concentration of chemical compounds", are summarized for each compound and indoor source: the ratios resulted larger than 1 for 32 of the 54 (59%) compounds detected, in other words, assuming constant mass fraction of the chemical compounds over the entire particle size range, the dose received by exposed persons would be underestimated. For some compounds the ratios resulted much larger than 1 (e.g. 3.3 for As in the case of mosquito coil combustion), then likely resulting in a significant underestimate of the actual dose. The reason for the large deviation between the two approaches (size-segregated mass fraction vs. constant mass fraction) is due to the deposition fractions (alveolar and tracheobronchial) of the particles which present a peak in the ultrafine range. Thus, chemical compounds with a significant contribution in that size range will present a higher deviation with respect to the dose evaluated considering a constant mass fraction. The As emitted by mosquito coil combustion is the most critical example: its contribution is mostly due to the size range 16.7–31.3 nm (Fig. 2a) where the deposition fraction is around 60%; indeed, the deposited concentration of As (with respect to the total concentration of As), when applying the size-resolved approach, resulted equal to 59%; on the contrary, considering the constant mass fraction (2.93×10^{-6}, Table 2), the deposited concentration of As was 18% of the total concentration of As (then, the ratio is 3.3).

Despite the key findings provided in the study and the related very important implications, the reader should be aware of the criticalities and limitations of the study in terms of both methodological assumptions and result exploitability.

As concerns the methodology, we point out that, mass fractions of HMs and PAHs were calculated considering PM_{10} concentration measured by the ELPI + ™: despite good agreement was found in previous studies with gravimetric measurements[73,74], the mass concentration it provides is an indirect estimate as it starts from the measurement of the particle number distribution. Thus, a larger uncertainty is expected with respect to the measurement of the particle mass concentration through the reference method (i.e. gravimetric method[75]). Nonetheless, in the experimental setup we adopted it was actually not possible, for practical reasons, to perform a parallel gravimetric sampling in the chamber.

Concerning the data exploitability, we highlight that the results we provided cannot be considered immediately applicable to other similar sources, indeed, the composition of the sources (e.g. additives to obtain a specific fragrance, scent, etc.) can strongly affect the emission of particle-bound compounds[39–41]. This is even more critical for cooking activities due to the abovementioned several influence parameters[43,45,63] affecting the emission: considering all the possible cooking types and foods would have been unfeasible. Moreover, the cooking experiments would have been critical also from a methodological perspective, indeed, differently from other sources (that were left to burn with no handling needed), food preparation needs frequent handling, and its duration is shorter than other combustion sources here tested.

Future developments of the study should then be focused on trying to extend the analysis here performed to different compositions/types of the indoor sources here investigated (e.g. including different compositions,

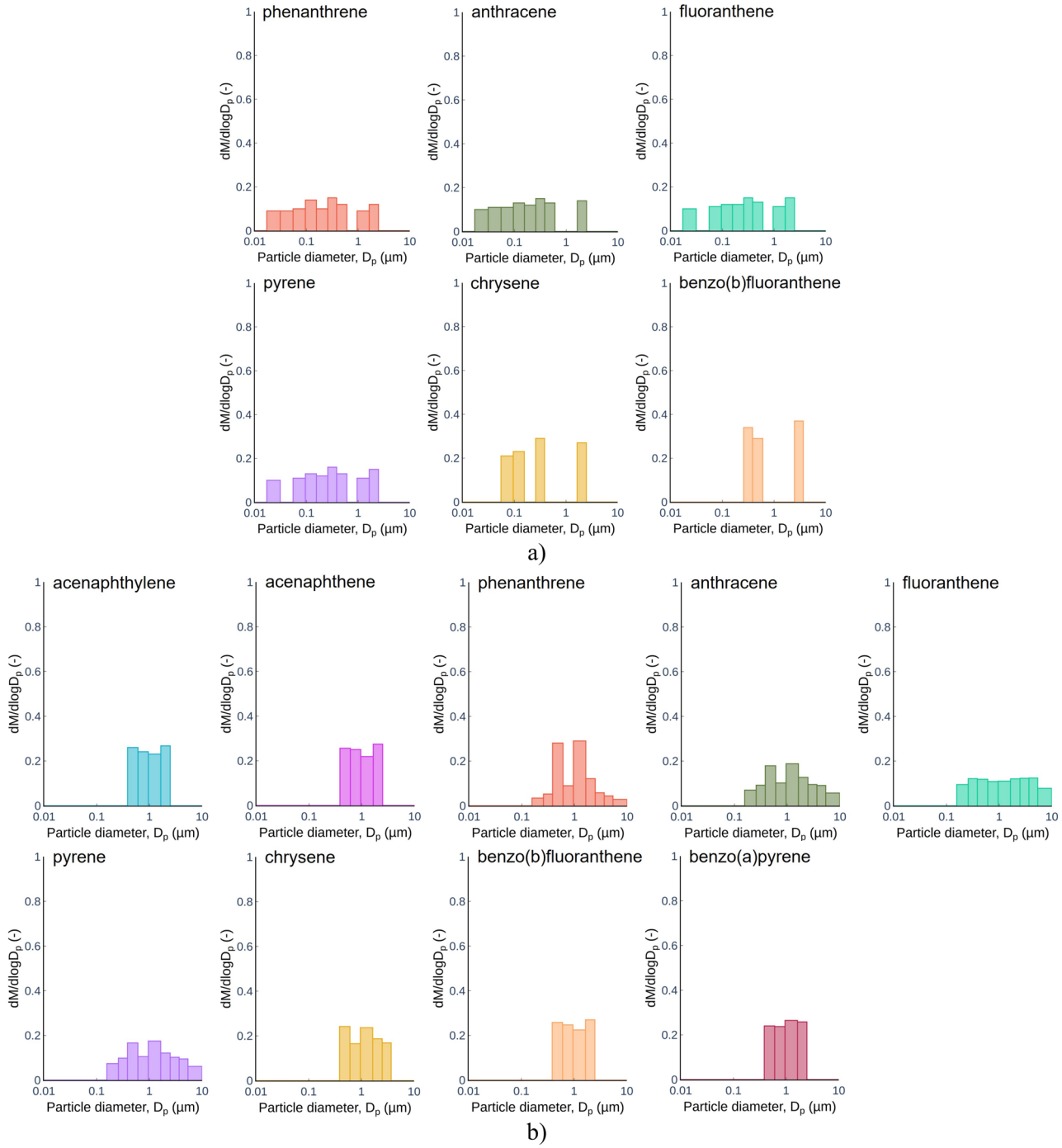

Fig. 5. Mass distributions (normalized to the total concentration) of PAHs in freshly emitted particles from candle (**a**), incense (**b**), mosquito coil combustions (**c**) and grilling bacon (**d**) (Sampling 2).

fragrances, scents of candles, mosquito coils, incenses as well as cooking activities with different stoves, foods, preparations). Moreover, in view of prospective risk analyses due to the exposure to indoor combustion sources, risk models able to account for the size-dependent chemical composition should be carried out. Indeed, to date, a lung cancer risk model able to take into account for the contribution of sub-micrometric particles was recently developed[32], but it is still based on the assumption of chemical composition invariant to the particle size (constant mass fraction); it should be properly modified to include the size-dependent mass-fraction.

Conclusions

In the present paper for the very first time the size-resolved chemical characterization of airborne particles freshly emitted by widely used indoor sources, i.e. incenses, candles, mosquito-coils and cooking activities (grilling bacon), was carried out. In particular, size-dependent particle-bound heavy metal and polycyclic aromatic

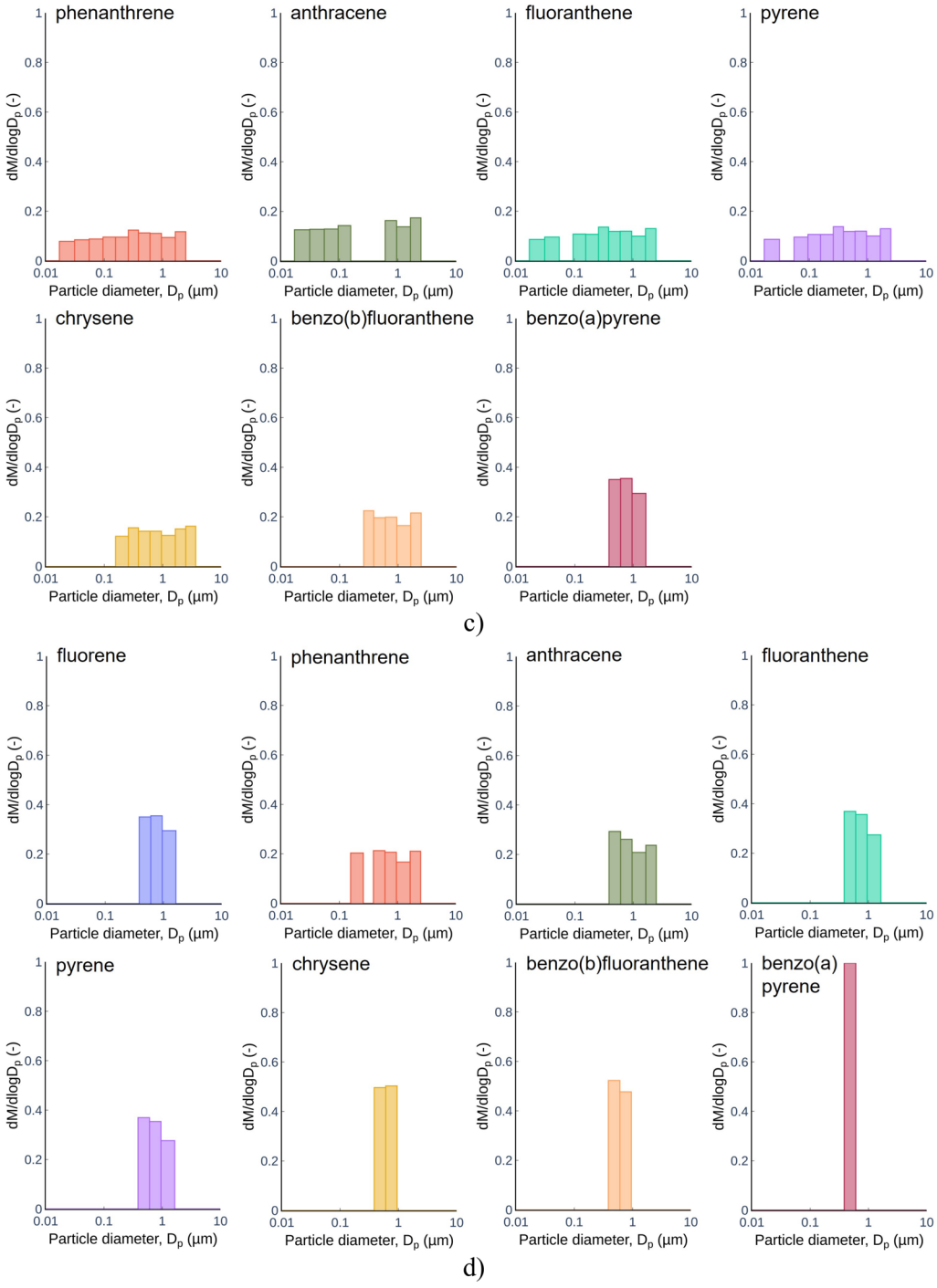

Fig. 5. (continued)

hydrocarbon contributions to the PM_{10} were provided thanks to a particle collection through an electric low-pressure impactor and consequent gas chromatography-mass spectrometry (GC–MS) and atomic emission spectrometry (AES) analyses.

The results of the study revealed that all the sources emit fresh particles with a significant contribution of PM_1 fraction (with respect to PM_{10}).

As concerns the heavy metal chemical analysis, Group 1 carcinogenic compounds (Cd, Cr(VI), As, and Ni) were only found in particle samples from mosquito coil combustion and grilling bacon. The calculated mass fractions were not negligible as they were mostly in the 10^{-6}–10^{-5} range and, moreover, the contribution of sub-micrometric particles to the total mass of emitted heavy metals was found extremely high: as an example, As, Ni, Cr(VI) emitted by the mosquito coils were almost exclusively due to the sub-micrometric particle range as well as As, Cd, and Cr(VI) emitted by grilling bacon.

	Candles	Incenses	Mosquito coils	Grilling bacon
HMs				
As	–	–	3.3	1.4
Cd	–	–	1.0	1.4
Cr(VI)	–	–	1.1	2.1
Ni	–	–	1.1	–
Pb	1.6	1.5	1.0	1.6
Sb	1.7	1.5	1.4	1.3
Cu	1.5	1.4	1.1	1.4
Zn	1.5	1.4	1.0	1.7
Co	–	–	–	2.3
Mn	1.2	–	–	–
PAHs				
Acenaphthylene		1.0		
Acenaphthene		1.0		
Fluorene				1.0
Phenanthrene	2.0	1.0	1.6	1.0
Anthracene	2.1	1.0	1.8	1.0
Fluoranthene	1.9	1.0	1.5	1.0
Pyrene	1.9	1.0	1.5	1.0
Benzo(a)anthracene				
Chrysene	1.8	1.0	1.0	1.0
Benzo(b)fluoranthene	1.2	1.0	1.0	1.0
Benzo(k)fluoranthene				
Benzo(a)pyrene		1.0	1.0	
Indeno(1,2,3-cd)pyrene				
Dibenzo(a,h)anthracene				
Benzo(g.h.i)perylene				

Table 4. Ratios between the deposited concentrations of chemical compounds (for each source) evaluated according the two different approaches adopted to estimate the mass fractions of chemical compounds: size resolved mass fraction and constant mass fraction.

In terms of PAHs, different compounds, including Group 1 (i.e. benzo(a)pyrene) and Group 2 carcinogenic compounds, were found in the freshly-emitted particles of the investigated sources with mass fraction in the 10^{-7}–10^{-5} range. A high contribution of sub-micrometric range was detected for most of the investigated PAHs.

The main implication of the results here shown is the possible underestimation of deposited concentration of chemical compounds (and then of the related dose of exposed people) when a constant mass fraction over the entire size range is adopted. Indeed, we showed that by adopting a constant mass fraction, instead of a size-dependent mass fraction of the compound here obtained, the deposited concentrations of chemical compounds were mostly underestimated: such underestimation resulted by a factor of 3 if the amount of the compound is mostly located in the ultrafine range (as we found for the As due to mosquito coil combustion).

The information provided can be extremely useful for detailed health risk assessments since they allow avoiding oversimplified assumptions based on considering the chemical composition of the emitted particles invariant to the particle size.

Data availability

The datasets used and/or analysed during the current study available from the corresponding author on reasonable request.

Received: 2 March 2024; Accepted: 22 August 2024
Published online: 05 September 2024

References

1. Dai, X., Shang, W., Liu, J., Xue, M. & Wang, C. Achieving better indoor air quality with IoT systems for future buildings: Opportunities and challenges. *Sci. Total Environ.* **895**, 164858 (2023).
2. Tham, K. W. Indoor air quality and its effects on humans—A review of challenges and developments in the last 30 years. *Energy Build.* **130**, 637–650 (2016).
3. Zhao, B., Shi, S. & Ji, J. S. The WHO Air Quality Guidelines 2021 promote great challenge for indoor air. *Sci. Total Environ.* **827**, 154376 (2022).
4. Kempton, L., Daly, D., Kokogiannakis, G. & Dewsbury, M. A rapid review of the impact of increasing airtightness on indoor air quality. *J. Build. Eng.* **57**, 104798 (2022).

5. Nabinger, S. & Persily, A. Impacts of airtightening retrofits on ventilation rates and energy consumption in a manufactured home. *Energy Build.* **43**, 3059–3067 (2011).
6. Stabile, L., Buonanno, G., Frattolillo, A. & Dell'Isola, M. The effect of the ventilation retrofit in a school on CO2, airborne particles, and energy consumptions. *Build. Environ.* **156**, 1–11 (2019).
7. Wei, G. *et al.* A review and comparison of the indoor air quality requirements in selected building standards and certifications. *Build. Environ.* **226**, 109709 (2022).
8. Calitz, A. P., Cullen, M. D. M. & Odendaal, F. Creating environmental awareness using an eco-feedback application at a higher education institution. *Southern Afr. J. Environ. Educ.* **36**, (2020).
9. Caracci, E., Canale, L., Buonanno, G. & Stabile, L. Effectiveness of eco-feedback in improving the indoor air quality in residential buildings: Mitigation of the exposure to airborne particles. *Build. Environ.* **226**, 109706 (2022).
10. Ali, M. U. *et al.* Pollution characteristics, mechanism of toxicity and health effects of the ultrafine particles in the indoor environment: Current status and future perspectives. *Crit. Rev. Environ. Sci. Technol.* **52**, 436–473 (2022).
11. Clifford, S. *et al.* Effects of exposure to ambient ultrafine particles on respiratory health and systemic inflammation in children. *Environ. Int.* **114**, 167–180 (2018).
12. Glencross, D. A., Ho, T.-R., Camina, N., Hawrylowicz, C. M. & Pfeffer, P. E. Air pollution and its effects on the immune system. *Free Radical Biol. Med.* **151**, 56–68 (2020).
13. Cassee, F. R., Héroux, M.-E., Gerlofs-Nijland, M. E. & Kelly, F. J. Particulate matter beyond mass: Recent health evidence on the role of fractions, chemical constituents and sources of emission. *Inhalation Toxicol.* **25**, 802–812 (2013).
14. Giechaskiel, B., Alföldy, B. & Drossinos, Y. A metric for health effects studies of diesel exhaust particles. *J. Aerosol Sci.* **40**, 639–651 (2009).
15. Kwon, H.-S., Ryu, M. H. & Carlsten, C. Ultrafine particles: Unique physicochemical properties relevant to health and disease. *Exp. Mol. Med.* **52**, 318–328 (2020).
16. Lin, S. *et al.* Particle surface area, ultrafine particle number concentration, and cardiovascular hospitalizations. *Environ. Pollut.* **310**, 119795 (2022).
17. Sager, T. M. & Castranova, V. Surface area of particle administered versus mass in determining the pulmonary toxicity of ultrafine and fine carbon black: Comparison to ultrafine titanium dioxide. *Part. Fibre Toxicol.* **6**, 15–15 (2009).
18. Schmid, O. & Stoeger, T. Surface area is the biologically most effective dose metric for acute nanoparticle toxicity in the lung. *J. Aerosol Sci.* **99**, 133–143 (2016).
19. Jiries, A. Vehicular contamination of dust in Amman, Jordan. *Environmentalist* **23**, 205–210 (2003).
20. Kumari, S., Jain, M. K. & Elumalai, S. P. Assessment of pollution and health risks of heavy metals in particulate matter and road dust along the road network of Dhanbad, India. *J. Health Pollut.* **11**, 210305 (2021).
21. Saeedi, M., Li, L. Y. & Salmanzadeh, M. Heavy metals and polycyclic aromatic hydrocarbons: Pollution and ecological risk assessment in street dust of Tehran. *J. Hazard. Mater.* **227**, 9–17 (2012).
22. Sakunkoo, P. *et al.* Human health risk assessment of PM(2.5)-bound heavy metal of anthropogenic sources in the Khon Kaen Province of Northeast Thailand. *Heliyon* **8**, e09572 (2022).
23. Castel, R. *et al.* Toward an interdisciplinary approach to assess the adverse health effects of dust-containing polycyclic aromatic hydrocarbons (PAHs) and metal (loid) s on preschool children. *Environ. Pollut.* **336**, 122372 (2023).
24. Låg, M., Øvrevik, J., Refsnes, M. & Holme, J. A. Potential role of polycyclic aromatic hydrocarbons in air pollution-induced non-malignant respiratory diseases. *Respir. Res.* **21**, 299 (2020).
25. Safo-Adu, G., Attiogbe, F., Emahi, I. & Ofosu, F. G. A review of the sources, distribution sequences, and health risks associated with exposure to atmospheric polycyclic aromatic hydrocarbons. *Cogent Eng.* **10**, 2199511 (2023).
26. International Agency for Research on Cancer. *IARC: Outdoor Air Pollution a Leading Environmental Cause of Cancer Deaths*. (2013).
27. Smichowski, P. & Gómez, D. R. An overview of natural and anthropogenic sources of ultrafine airborne particles: Analytical determination to assess the multielemental profiles. *Appl. Spectrosc. Rev.* **59**, 1–27 (2023).
28. Li, X., Cai, R., Hao, J., Smith, J. N. & Jiang, J. Online detection of airborne nanoparticle composition with mass spectrometry: Recent advances, challenges, and opportunities. *TrAC Trends Anal. Chem.* 117195 (2023).
29. López, M. *et al.* Size-resolved chemical composition and toxicity of particles released from refit operations in shipyards. *Sci. Total Environ.* **880**, 163072 (2023).
30. Buonanno, G., Giovinco, G., Morawska, L. & Stabile, L. Lung cancer risk of airborne particles for Italian population. *Environ. Res.* **142**, 443–451 (2015).
31. Caracci, E., Stabile, L. & Buonanno, G. A simplified approach to evaluate the lung cancer risk related to airborne particles emitted by indoor sources. *Build. Environ.* **204**, 108143 (2021).
32. Sze-To, G. N., Wu, C. L., Chao, C. Y. H., Wan, M. P. & Chan, T. C. Exposure and cancer risk toward cooking-generated ultrafine and coarse particles in Hong Kong homes. *HVAC&R Res.* **18**, 204–216 (2012).
33. Mulla, M. S., Thavara, U., Tawatsin, A., Kong-Ngamsuk, W. & Chompoosri, J. Mosquito burden and impact on the poor: Measures and costs for personal protection in some communities in Thailand. *J. Am. Mosquito Control Assoc.* **17**, 153–159 (2001).
34. Pacitto, A. *et al.* Daily submicron particle doses received by populations living in different low- and middle-income countries. *Environ. Pollut.* **269**, 116229 (2021).
35. Taiwo Idowu, E., Aimufua, O. J., Yomi-Onilude, E., Akinsanya, B. & Adetoro Otubanjo, O. Toxicological effects of prolonged and intense use of mosquito coil emission in rats and its implications on malaria control. *Revista de biologia tropical* **61**, 1463–1473 (2013).
36. Lee, S. C. & Wang, B. Characteristics of emissions of air pollutants from burning of incense in a large environmental chamber. *Atmosp. Environ.* **38**, 941–951 (2004).
37. See, S. W. & Balasubramanian, R. Characterization of fine particle emissions from incense burning. *Build. Environ.* **46**, 1074–1080 (2011).
38. Afshari, A., Matson, U. & Ekberg, L. E. Characterization of indoor sources of fine and ultrafine particles: A study conducted in a full-scale chamber. *Indoor Air* **15**, 141–150 (2005).
39. Pagels, J. *et al.* Chemical composition and mass emission factors of candle smoke particles. *J. Aerosol. Sci.* **40**, 193–208 (2009).
40. Stabile, L., Fuoco, F. C. & Buonanno, G. Characteristics of particles and black carbon emitted by combustion of incenses, candles and anti-mosquito products. *Build. Environ.* **56**, 184–191 (2012).
41. Derudi, M. *et al.* Emissions of air pollutants from scented candles burning in a test chamber. *Atmosp. Environ.* **55**, 257–262 (2012).
42. Buonanno, G., Johnson, G., Morawska, L. & Stabile, L. Volatility characterization of cooking-generated aerosol particles. *Aerosol. Sci. Technol.* **45**, 1069–1077 (2011).
43. Buonanno, G., Morawska, L. & Stabile, L. Particle emission factors during cooking activities. *Atmosp. Environ.* **43**, 3235–3242 (2009).
44. Ma, S., Liu, W., Meng, C., Dong, J. & Zhang, S. Temperature-dependent particle mass emission rate during heating of edible oils and their regression models. *Environ. Pollut.* **323**, 121221 (2023).
45. See, S. W. & Balasubramanian, R. Physical characteristics of ultrafine particles emitted from different gas cooking methods. *Aerosol. Air Qual. Res.* **6**, 82–92 (2006).

46. Tang, R. & Pfrang, C. Indoor particulate matter (PM) from cooking in UK students' studio flats and associated intervention strategies: Evaluation of cooking methods, PM concentrations and personal exposures using low-cost sensors. *Environ. Sci. Atmos.* **3**, 537–551 (2023).
47. Wallace, L. A., Emmerich, S. J. & Howard-Reed, C. Source strengths of ultrafine and fine particles due to cooking with a gas stove. *Environ. Sci. Technol.* **38**, 2304–2311 (2004).
48. Fang, G. C. *et al.* Fine (PM2.5), coarse (PM2.5–10), and metallic elements of suspended particulates for incense burning at Tzu Yun Yen temple in central Taiwan. *Chemosphere* **51**, 983–991 (2003).
49. Hu, M. T. *et al.* Characteritization of, and health risks from, polychlorinated dibenzo-p-dioxins/dibenzofurans from incense burned in a temple. *Sci. Total Environ.* **407**, 4870–4875 (2009).
50. Ji, X. *et al.* Characterization of particles emitted by incense burning in an experimental house. *Indoor Air* **20**, 147–158 (2010).
51. Orecchio, S. Polycyclic aromatic hydrocarbons (PAHs) in indoor emission from decorative candles. *Atmosp. Environ.* **45**, 1888–1895 (2011).
52. Roy, A. A., Baxla, S. P., Gupta, T., Bandyopadhyaya, R. & Tripathi, S. N. Particles emitted from indoor combustion sources: Size distribution measurement and chemical analysis. *Inhalat. Toxicol.* **21**, 837–848 (2009).
53. Yang, T.-T., Lin, S.-T., Lin, T.-S. & Chung, H.-Y. Characterization of polycyclic aromatic hydrocarbon emissions in the particulate and gas phase from smoldering mosquito coils containing various atomic hydrogen/carbon ratios. *Sci. Total Environ.* **506**, 391–400 (2015).
54. Yang, T. T., Lin, S. T., Hung, H. F., Shie, R. H. & Wu, J. J. Effect of relative humidity on polycyclic aromatic hydrocarbon emissions from smoldering incense. *Aerosol. Air Qual. Res.* **13**, 662–671 (2013).
55. Zhang, L. *et al.* Using charcoal as base material reduces mosquito coil emissions of toxins. *Indoor Air* **20**, 176–184 (2010).
56. Zhou, W. *et al.* Metals, PAHs and oxidative potential of size-segregated particulate matter and inhalational carcinogenic risk of cooking at a typical university canteen in Shanghai, China. *Atmosp. Environ.* **287**, 119250 (2022).
57. Cui, S., Cohen, M., Stabat, P. & Marchio, D. CO2 tracer gas concentration decay method for measuring air change rate. *Build. Environ.* **84**, 162–169 (2015).
58. Cheng, Y. S., Bechtold, W. E., Yu, C. C. & Hung, I. F. Incense smoke: Characterization and dynamics in indoor environments. *Aerosol. Sci. Technol.* **23**, 271–281 (1995).
59. Nazaroff, W. W. Indoor particle dynamics. *Indoor Air Suppl.* **14**, 175–183 (2004).
60. Patel, S. *et al.* Indoor particulate matter during HOMEChem: Concentrations, size distributions, and exposures. *Environ. Sci. Technol.* **54**, 7107–7116 (2020).
61. Virtanen, A., Marjamäki, M., Ristimäki, J. & Keskinen, J. Fine particle losses in electrical low-pressure impactor. *J. Aerosol. Sci.* **32**, 389–401 (2001).
62. International Commission on Radiological Protection. Human respiratory tract model for radiological protection. A report of a Task Group of the International Commission on Radiological Protection. *Annals of the ICRP* **24**, 1–482 (1994).
63. See, S. W. & Balasubramanian, R. Risk assessment of exposure to indoor aerosols associated with Chinese cooking. *Environ. Res.* **102**, 197–204 (2006).
64. Buonanno, G., Stabile, L., Morawska, L., Giovinco, G. & Querol, X. Do air quality targets really represent safe limits for lung cancer risk?. *Sci. Total Environ.* **580**, 74–82 (2017).
65. Pacitto, A. *et al.* Particle-related exposure, dose and lung cancer risk of primary school children in two European countries. *Sci. Total Environ.* **616–617**, 720–729 (2018).
66. See, S. W. & Balasubramanian, R. Chemical characteristics of fine particles emitted from different gas cooking methods. *Atmosp. Environ.* **42**, 8852–8862 (2008).
67. Lin, T.-S. Indoor Air Pollution: Unusual Sources. in *Encyclopedia of Environmental Health* 201–207 (2011). https://doi.org/10.1016/B978-0-444-52272-6.00710-8.
68. Stabile, L., Buonanno, G., Avino, P., Frattolillo, A. & Guerriero, E. Indoor exposure to particles emitted by biomass-burning heating systems and evaluation of dose and lung cancer risk received by population. *Environ. Pollut.* **235**, 65–73 (2018).
69. Office of Environmental Health Hazard Assessment. *Technical Support Document for Cancer Potency Factors: Methodologies for Derivation, Listing of Available Values, and Adjustments to Allow for Early Life Stage Exposures. California Environmental Protection Agency* (2009).
70. Martins, V. *et al.* Relationship between indoor and outdoor size-fractionated particulate matter in urban microenvironments: Levels, chemical composition and sources. *Environ. Res.* **183**, 109203 (2020).
71. Pekey, B. *et al.* Indoor/outdoor concentrations and elemental composition of PM10/PM2.5 in urban/industrial areas of Kocaeli City, Turkey. *Indoor Air* **20**, 112–125 (2010).
72. Sánchez-Piñero, J. *et al.* Inhalation bioaccessibility estimation of polycyclic aromatic hydrocarbons from atmospheric particulate matter (PM10): Influence of PM10 composition and health risk assessment. *Chemosphere* **263**, (2021).
73. Held, A. *et al.* Aerosol size distributions measured in urban, rural and high-alpine air with an electrical low pressure impactor (ELPI). *Atmosp. Environ.* **42**, 8502–8512 (2008).
74. Maricq, M. M., Xu, N. & Chase, R. E. Measuring particulate mass emissions with the electrical low pressure impactor. *Aerosol. Sci. Technol.* **40**, 68–79 (2006).
75. Buonanno, G., Dell'Isola, M., Stabile, L. & Viola, A. Critical aspects of the uncertainty budget in the gravimetric PM measurements. *Measurement* **44**, 139–147 (2010).

Acknowledgements

This perspective was supported by Project ECS 0000024 "Ecosistema dell'innovazione—Rome Technopole" financed by EU in NextGenerationEU plan through MUR Decree n. 1051 23.06.2022 PNRR Missione 4 Componente 2 Investimento 1.5—CUP H33C22000420001.

Author contributions

L.S., P.A. M.C, and G.B. designed the experimental set up and tested the experimental set up. E.C., A.I., F.C., and I.N., performed the experiments. L.S. and G.B. directly supervised the experiments. E.C., L.S., P.A., M.C. A.M. and S.P. analyzed the data. E.C., L.S., A.I., and F.C. wrote the manuscript. G.B, P.A., and M.C. revised the manuscript.

Competing interests

The authors declare no competing interests.

Additional information

Supplementary Information The online version contains supplementary material available at https://doi.org/10.1038/s41598-024-70978-3.

Correspondence and requests for materials should be addressed to L.S.

Reprints and permissions information is available at www.nature.com/reprints.

Publisher's note Springer Nature remains neutral with regard to jurisdictional claims in published maps and institutional affiliations.